Improved Analytical Modeling of Membrane Large Deflection With Lateral Force for the Underwater CMUT Based on Von Kármán Equations

Jiujiang Wang, *Student Member, IEEE*, Sio Hang Pun, *Member, IEEE*, Peng Un Mak, *Senior Member, IEEE*, Ching-Hsiang Cheng, *Member, IEEE*, Yuanyu Yu, *Student Member, IEEE*, Pui-In Mak, *Senior Member, IEEE*, and Mang I Vai, *Senior Member, IEEE*

***Abstract*— This paper is to develop analytical models for the underwater capacitive micromachined ultrasonic transducer (CMUT) to understand its large deflection effect from the water pressure. To accurately model the displacement profile of the CMUT under the water pressure, Von Kármán equations and the perturbation method are employed to calculate the membrane deformation from a uniform pressure. The equations for an annular-ring plate model are first applied to calculate the displacement profile of the uniform CMUT membrane. The lateral force due to the membrane elongation is considered in the proposed model, which is used to calculate the displacement profiles for both conventional and collapse mode CMUTs under different external pressures. When compared with finite-element method results, the proposed model can predict the displacement profiles of the conventional-mode CMUT under water pressure ranging from 0.8 to 4 MPa with an error of <1%. It can also estimate CMUT membrane that operates in collapse mode with an error in the deflection profile for <4.7% from 5 to 14 MPa. In addition, it is worth to mention that the proposed model can cover the small deflection scenarios but with relatively larger error under collapse mode.**

***Index Terms*— CMUT, lateral force, perturbation method, Von Kármán equations.**

Manuscript received August 20, 2015; revised May 24, 2016; accepted June 26, 2016. Date of publication July 7, 2016; date of current version August 3, 2016. This work was supported in part by the Research Committee of University of Macau under Grant MRG014/MPU/2014/FST, Grant MYRG2014-00010-AMSV, Grant MYRG103(Y1-L3)-FST13-VMI, Grant MYRG079(Y1-L2)-FST12-VMI, and Grant MYRG076(Y1-L2)-FST12-MPU and in part by the Science and Technology Development Fund (FDCT) of Macau under Grant 087/2012/A3 and Grant 047/2013/A2. The associate editor coordinating the review of this paper and approving it for publication was Dr. Anupama Kaul.

J. Wang, Y. Yu, P.-I. Mak, and M. I Vai are with the State Key Laboratory of Analog and Mixed-Signal VLSI, University of Macau, Macau 999078, China, and also with the Department of Electrical and Computer Engineering, Faculty of Science and Technology, University of Macau, Macau 999078, China (e-mail: tswangjade@gmail.com; yuyuanyu@gmail.com; pimak@umac.mo; fstmiv@umac.mo).

S. H. Pun is with the State Key Laboratory of Analog and Mixed-Signal VLSI, University of Macau, Macau 999078, China (e-mail: lodgepun@umac.mo).

P. U. Mak is with the Department of Electrical and Computer Engineering, Faculty of Science and Technology, University of Macau, Macau 999078, China (e-mail: fstpum@umac.mo).

C.-H. Cheng is with the State Key Laboratory of Analog and Mixed-Signal VLSI, University of Macau, Macau 999078, China, and also with the Department of Industrial and Systems Engineering, The Hong Kong Polytechnic University, Hong Kong, China (e-mail: ching-hsiang.cheng@polyu.edu.hk).

Digital Object Identifier 10.1109/JSEN.2016.2586969

I. Introduction

TODAY, owing to the increasing needs for searching the natural resources in the ocean, the exploration of ocean is further reaching out from off-shore to the deep sea. The probing and measuring techniques in the deep water are more challenging due to a higher water pressure and lower visibility in the water with turbulent flow. The former problem can be overcome by using a pressurized underwater vehicle and the latter can be tackled by employing an ultrasonic imaging system, where the long visual distance in the turbulent water makes ultrasonic imaging suitable for underwater inspection, as well as objects differentiation and classification [1] for a variety of applications in scientific, commercial and military purposes [2]. Based on the current technology, 2-D and 3-D images can be acquired using 1-D and 2-D transducer arrays [3].

A capacitive micromachined ultrasonic transducer (CMUT) is a miniaturized ultrasound generator and detector as an alternative for the traditional piezoelectric transducer. Basically, a CMUT is like a parallel-plate capacitor with a membrane as the top electrode, and a silicon substrate as the bottom electrode of the capacitor, where a cavity is sandwiched in between the two electrodes to allow the vibration of the membrane to generate and receive ultrasound. Current CMUTs are mostly fabricated by using the microfabrication technique to ease the integration to the electronic circuits. Since the first introduction of CMUTs, they have been used for both airborne and underwater areas in recent two decades [4], [5]. When applying an AC voltage between the top and bottom electrodes, the generated electrostatic force causes the membrane (with the top electrode) to vibrate against the substrate to generate ultrasound; vice versa, an incoming ultrasound can also vibrate the membrane to generate an AC signal for ultrasonic detection. In addition to the ultrasonic imaging, blood and intraocular pressure measurements can also use microsensors, therefore, CMUTs can be used to measure blood pressure, or the thickness of the cornea and the intraocular pressure simultaneously [6]–[8].

CMUTs can work in conventional and also collapse modes depending on different DC biases [9]. When operating in conventional mode, the membrane is not in contact with the substrate, which allows the whole membrane to vibrate for generating larger deflection that can generate more output pressure [10]. When operating in collapse mode, a higher DC bias is applied to pull in the center of the membrane to be in contact with the substrate, therefore, only the off-center portions of the membrane is movable for ultrasound sensing and generating. Both simulation and experimental results show that the transmitting output pressure and also the receiving sensitivity of the collapse mode is higher than that of the conventional mode [11], [12]. Under normal circumstances when operating at one atmospheric pressure, for example, for medical applications, the membrane can work in both modes by using the DC bias to switch from one to another. However, for underwater application in the deep ocean, such as autonomous underwater vehicles (AUV), CMUTs may require to operate at about 500 meters below the sea level, where the water pressure exerted on the membrane is about 5 MPa such that the membrane will be in touch with the substrate during the operation. In this case, the CMUT can only operate in collapse mode without using a high DC bias to maintain the contact of the membrane to the substrate. To predict the behavior of the CMUT membrane, analytical formulation derivation, equivalent circuit model (ECM), and finite element method (FEM) are commonly used modeling and simulation techniques. In 2001, Bayram *et al.* reported the collapse mode operation by simulating the effects of different electrode parameters at the collapse voltage using ANSYS [13]. Nikoozadeh *et al.* used an iteration method to calculate the collapse voltage, which also mentioned that the lateral force should be considered in order to achieve more accurate results [14]. Alternately, Olcum *et al.* employed an ECM to simulate the mechanical behavior of the membrane under small and large deformations [15]. FEM has been commonly used to simulate the behavior of CMUTs, however, the computational resource required to perform an accurate FEM simulation can be inevitably large [16]–[19].

When the maximum displacement of the membrane is less than 20% of its thickness, it is considered as small deformation [20], which has been well studied by the prior researchers [16], [21]–[23]. When the maximum displacement of the membrane is comparable with or larger than its thickness, it is said to operate in large deformation [20], the effect of the membrane elongation is significant [14], [24], and the lateral force is necessary to be considered in the modeling of the membrane deflection of CMUTs. To the best of our knowledge, there is still no analytical expression for the membrane deflection profile for collapse mode CMUTs [25].

Therefore, in this study, we proposed to employ Von Kármán equations, which were commonly used in solving the general plate problems [26]–[28], to include the lateral force when modeling the membrane deflection of an underwater CMUT.

The rest of the article was arranged as follows. In Section II, the methods to define the model of the membrane deflection were first discussed. Then, the use of the model for predicting the membrane deflections of the conventional and collapse mode CMUTs could be found in Section III. In Section IV, the results of the proposed model were compared with the results obtained by the FEM model. Finally, the conclusion of the article was drawn in Section V.

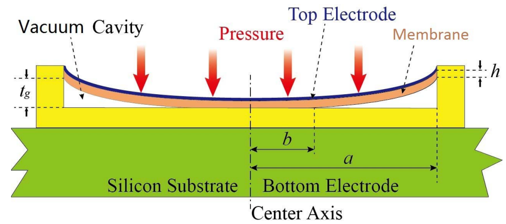

(a)

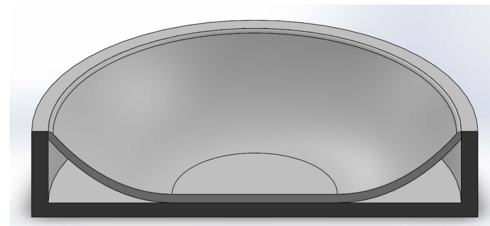

(b)

Fig. 1. (a) The cross-sectional view of a collapse CMUT. a is the radius of the membrane, b is radius of the collapse area, h is the membrane thickness and t_g is the vacuum gap height. (b) The cross-sectional perspective view of a collapse CMUT. The collapse area is in a circular shape at the center of membrane and the deflected portion is in an annular ring shape.

II. Methodology

Fig. 1 shows the cross-sectional and perspective views of a collapse CMUT with a circular membrane. It is composed of a substrate, a membrane, a top electrode and a vacuum gap, where a is the radius of the membrane, b is radius of the collapse area, when $b = 0$ it is in conventional mode, h is the membrane thickness, and t_g is the vacuum gap height. The substrate is generally much thicker than the membrane and is considered as a rigid body whose deformation can be ignored. It is highly doped and is mostly used as the bottom electrode of the CMUT. The top electrode is a thin layer of metallic conductor coated on the dielectric membrane, so it is part of the membrane to vibrate simultaneously during operation. When considering the deflection of the membrane, the thickness of the top electrode can be first assumed infinitesimally thin to simplify the problem. When a DC bias between the top and bottom electrodes or an external pressure (such as water pressure in deep sea) is applied, the membrane bends towards the substrate. This static deflection of the membrane defines the operation mode of the CMUT [29]. According to the previous researches, making the membrane to contact with the substrate in the collapse mode operation can achieve better output pressure when transmitting the ultrasound and also higher detection sensitivity when receiving the ultrasound [11], [12].

When deflection of the membrane is large, each infinitesimal small fragment of the membrane experiences a stretching force oriented in the radial direction as depicted in Fig. 2. In the figure, N_r represents the lateral force stretching the fragment and dN_r is the small increment of the lateral force at the opposite side of the fragment. By including the lateral

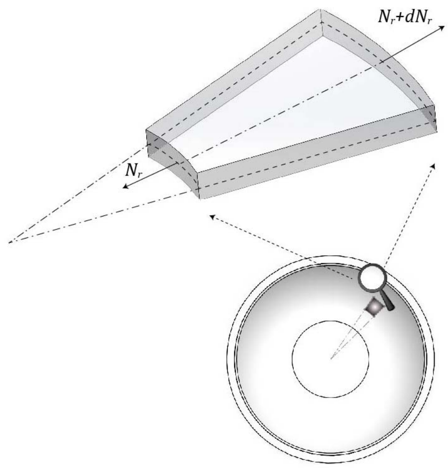

Fig. 2. Lateral force in a deformed membrane, with the magnification of the fragment in the deflected part.

force into the analysis of the CMUT membrane, supposing a uniform pressure q is exerted on the membrane, the equilibrium equations of the membrane fragment can be expressed as (1) and (2). The bending moment in radial direction M_r and in tangential direction M_t are represented as (3) and (4) respectively,

$$\frac{1}{r}\frac{\mathrm{d}M_t}{\mathrm{d}r}-\frac{1}{r}\frac{\mathrm{d}^2}{\mathrm{d}r^2}(rM_r)=q+\frac{1}{r}\frac{\mathrm{d}}{\mathrm{d}r}(N_r r\frac{\mathrm{d}\varpi}{\mathrm{d}r}) \tag{1}$$

$$\frac{\mathrm{d}}{\mathrm{d}r}(rN_r)-N_t=0 \tag{2}$$

$$M_r=-D\left[\frac{\mathrm{d}^2\varpi}{\mathrm{d}r^2}+\frac{\nu}{r}\frac{\mathrm{d}\varpi}{\mathrm{d}r}\right] \tag{3}$$

$$M_t=-D\left[\frac{1}{r}\frac{\mathrm{d}\varpi}{\mathrm{d}r}+\nu\frac{\mathrm{d}^2\varpi}{\mathrm{d}r^2}\right] \tag{4}$$

where ϖ depicts the displacement of the fragment, r is its radial position, ν is the Poisson's ratio of the membrane material. N_r and N_t represent the lateral force in radial direction and tangential direction respectively. By rearranging the terms, M_r and M_t could be eliminated and eventually, a compact equation set (5) & (6) was derived which was called Von Kármán equations [30]. For conventional mode CMUT which is a special case of the collapse mode when $b=0$, (7) is used instead of (6) [31].

$$r\frac{\mathrm{d}}{\mathrm{d}r}\frac{1}{r}\frac{\mathrm{d}}{\mathrm{d}r}(r^2N_r)=-\frac{1}{2}Eh\left(\frac{\mathrm{d}\varpi}{\mathrm{d}r}\right)^2 \tag{5}$$

$$Dr\frac{\mathrm{d}}{\mathrm{d}r}\frac{1}{r}\frac{\mathrm{d}}{\mathrm{d}r}\left(r\frac{\mathrm{d}\varpi}{\mathrm{d}r}\right)=rN_r\frac{\mathrm{d}\varpi}{\mathrm{d}r}+\frac{1}{2}q(r^2-b^2) \tag{6}$$

$$Dr\frac{\mathrm{d}}{\mathrm{d}r}\frac{1}{r}\frac{\mathrm{d}}{\mathrm{d}r}\left(r\frac{\mathrm{d}\varpi}{\mathrm{d}r}\right)=rN_r\frac{\mathrm{d}\varpi}{\mathrm{d}r}+\frac{1}{2}qr^2 \tag{7}$$

For collapse CMUTs, there is an additional boundary condition (8) for the collapse area, because the collapse area of the CMUT membrane has a different mechanical property as described in [30], where it was assumed to be a rigid circular disk without any deformation, but for this study, it has the same mechanical property as the deflected annular region.

$$u_0=\frac{r}{Eh}\left[\frac{\mathrm{d}}{\mathrm{d}r}(rN_r)-\nu N_r\right] \tag{8}$$

where E is the Young's Modulus of the membrane, and u_0 represents the elongation of the membrane at the collapse area. The flexural rigidity of the membrane D can be described as:

$$D=\frac{Eh^3}{12(1-\nu^2)} \tag{9}$$

The governing equations (5)-(6) for the large deflection CMUT can be solved with the perturbation method. It uses power series to approximate the solutions of equations, which is useful to solve some nonlinear differential equations that are not easy to derive for analytical solutions [32], [33]. According to the perturbation method, all independent variables should be re-expressed as dimensionless terms. Therefore, the external pressure q is expressed as a nondimensional variable, denoted as Q.

$$Q=\frac{3(1-\nu^2)\sqrt{3(1-\nu^2)}}{4}\frac{a^4q}{Eh^4} \tag{10}$$

Similarly, the lateral force N_r, the membrane displacement ϖ and radial position r are expressed as nondimensional variables S, W and x, respectively.

$$S=3(1-\nu^2)\frac{a^2N_r}{Eh^3} \tag{11}$$

$$W=\sqrt{3(1-\nu^2)}\frac{\varpi}{h} \tag{12}$$

$$x=1-\frac{r^2}{a^2} \tag{13}$$

Then, Q, S, and W are expressed as functions of W_m which is the perturbation parameter for solving the differential equations,

$$Q=\alpha_1W_m+\alpha_3W_m^3 \tag{14}$$

$$S=s_2(x)W_m^2 \tag{15}$$

$$W=w_1(x)W_m+w_3(x)W_m^3 \tag{16}$$

where α_1 and α_3 are coefficients of W_m to be solved later. $s_2(x)$, $w_1(x)$, and $w_3(x)$ are polynomial functions of x and are to be developed using the perturbation method. The relationship between the perturbation parameter W_m and the displacement at the position $r=b$ is defined by (17).

$$W_m=\sqrt{3(1-\nu^2)}\left[\frac{\varpi}{h}\right]_{r=b} \tag{17}$$

Now, the variables q, N_r, ϖ and r in (5) - (6) are replaced with nondimensional parameters Q, S, W and x in accordance with the relationships stated in (10) - (13). Also, the equation set (5) & (6) and boundary conditions are modified after x is introduced as the variable. The value of u_0 can be calculated as follows and will be used in solving $s_2(x)$ and $w_3(x)$.

$$u_0=\frac{h^2W_m^2}{6(a-b)(1-\nu^2)} \tag{18}$$

By rearranging the same order terms of W_m in the modified equations and boundary conditions, a new set of linear differential equations has been developed, the coefficients and the polynomials functions can be obtained and the ϖ is then

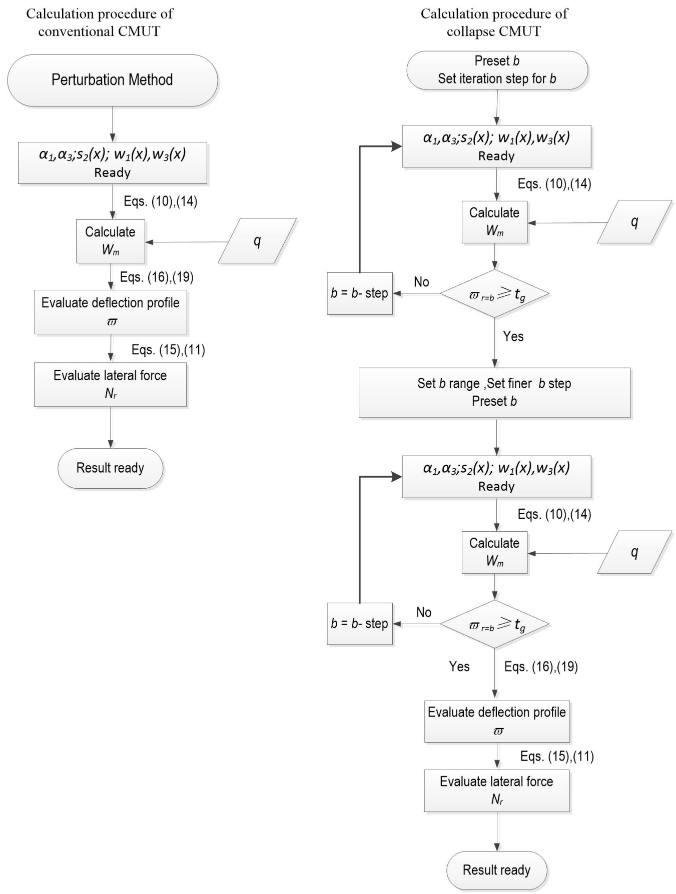

Fig. 3. The calculation procedure for the deflection profiles of the conventional and collapse CMUTs.

TABLE I

PARAMETERS OF THE CMUT WITH LARGE DEFLECTION OF THE MEMBRANE. THE PARAMETERS WERE ADOPTED FROM [15]

Parameters	Values
Membrane radius, a	30 μm
Membrane thickness, h	1.4 μm
Gap height, tg	1.4 μm
Young's Modulus, E	110 GPa
Poisson's ratio, ν	0.27
External pressure, q	0.8 MPa $\sim$ 4.0 MPa
Membrane material	Si_3N_4
Density of Si_3N_4	3.1 g/cm^3

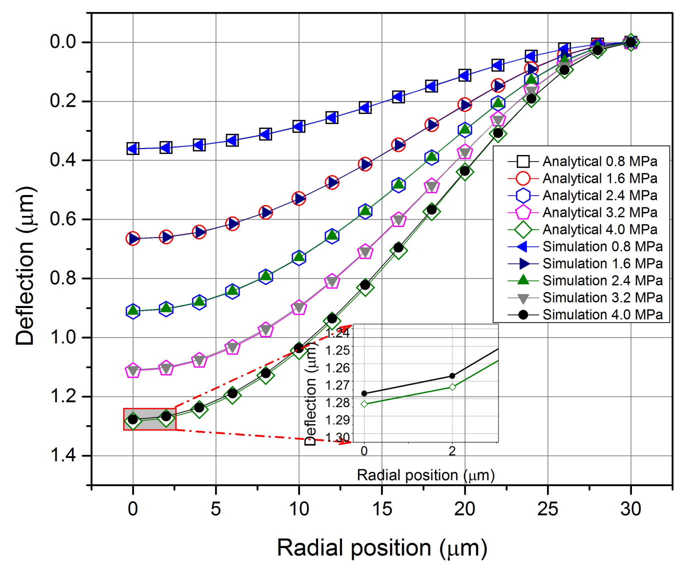

Fig. 4. Deflection profiles of the large deflection of membranes in conventional mode.

solved as (19), which gives the displacement profile of the CMUT membrane with large deformation.

$$\varpi = \frac{Wh}{\sqrt{3(1-\nu^2)}} \tag{19}$$

The displacement profile for conventional mode can be developed in a similar manner, and for the purpose of better understanding, the procedure of applying the proposed model for calculating the deflection profiles is summarized in Fig. 3.

III. MODEL VERIFICATIONS

In this section, by using the analytical solutions obtained in the previous section, the membrane displacement profiles for both conventional and collapse mode CMUTs under large deflection were calculated. The calculation results were also compared with the results from FEM simulation. The results of large deflection in conventional mode showed that the lateral force plays an important role in membrane deflection.

A. Conventional Mode CMUTs With Large Deflection of the Membrane

In this case, the membrane profiles of a conventional mode CMUT under external pressures were studied and its parameters are shown in Table I, which were adopted from [15], where the gap height was increased to 1.40 μm so that the deflections of the membrane were considered large and the external pressure was ranged from 0.8 MPa to 4 MPa to prevent the membrane touching the substrate.

By plugging the numbers into the model, all coefficients (α_1, α_3, W_m) and polynomial functions ($w_1(x)$, $w_3(x)$) were obtained and then substituted into (19) to get the displacement profile of the CMUT. The calculated membrane profiles of the CMUT under various external pressures (0.8 MPa $\sim$ 4.0 MPa) and the corresponding results from FEM are shown in Fig. 4, where its y-axis coincides with the perpendicular center-line of the CMUT membrane. The FEM simulations were performed by a commercial software COMSOL Multiphysics 4.4 (COMSOL, Inc., Stockholm, Sweden). Two 2D axisymmetric plates separated by air were used to represent the circular membrane and the substrate in *solid mechanics* physics domain. The dimensions and the material properties of the models were the same as in Table I. A *contact pair* was defined at the lower boundary of membrane and the upper boundary of substrate, and two *fixed constraints* were applied to the membrane boundary and the substrate. A boundary load representing the external load was applied uniformly on the membrane. Free triangular meshes with the maximum size of 0.7 μm were employed in the model. By using the *stationary* solver, the membrane defections under different

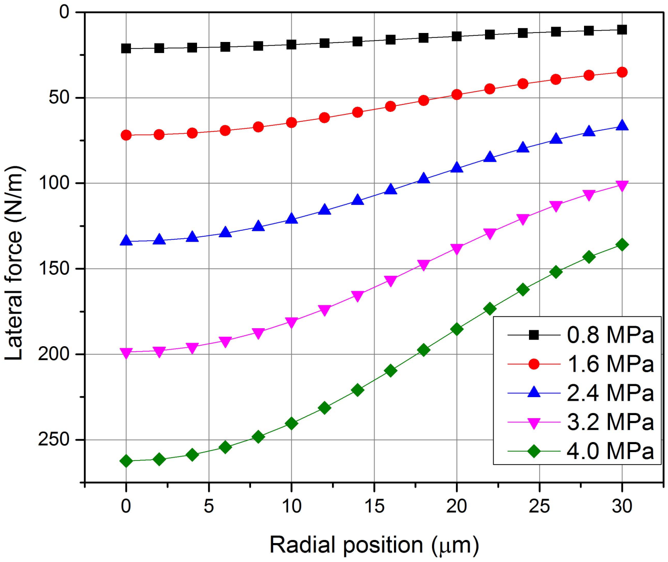

Fig. 5. Modeling results of lateral force for the large deflection membrane in conventional mode.

loads could be acquired. From our observation, the calculated results match well with the simulated results from FEM. The magnified window of Fig. 4 shows that the calculated result was very close to the simulation result. Overall, the maximum error between the calculation and simulation is less than 1% for all the selected situations. (The error percentage is evaluated by dividing the difference over the simulation result and herein after.)

Meanwhile, the calculated lateral forces of the membrane can be found in Fig. 5. The figure shows that the lateral force is non-linearly proportional to the deformation of the membrane and the largest lateral force appears at the center of the membrane with a 4.0 MPa external pressure, which has the highest deformation in reference to Fig. 4. And it can be found that the values of the lateral force increases significantly with the external pressures and these results show that the lateral force should not be neglected in the large deflection cases.

B. Collapse Mode CMUTs With Large Deflection of the Membrane

Another interesting operation mode of the CMUT is commonly known as collapse mode. The collapse of the membrane is presented in the developed model by the radius b to show the collapse region, which is caused by an external pressure or a DC bias voltage. For the collapse mode CMUT, the maximum membrane deflection is limited by the height of the vacuum cavity (gap height). Therefore, the ratio of the gap height to the membrane thickness can be used as a criterion to evaluate the deflection situation. For the purpose of consistency, the configuration of the CMUT is still defined in Table I but applying with higher external pressures (5 MPa $\sim$ 14 MPa) to collapse the membrane.

To simulate the collapse phenomena in the analytical model, an iterative method based on the developed model was performed by evaluating the radius b of the collapse area corresponding to the external pressure. In addition to b, the coefficients and the polynomial functions of the collapse

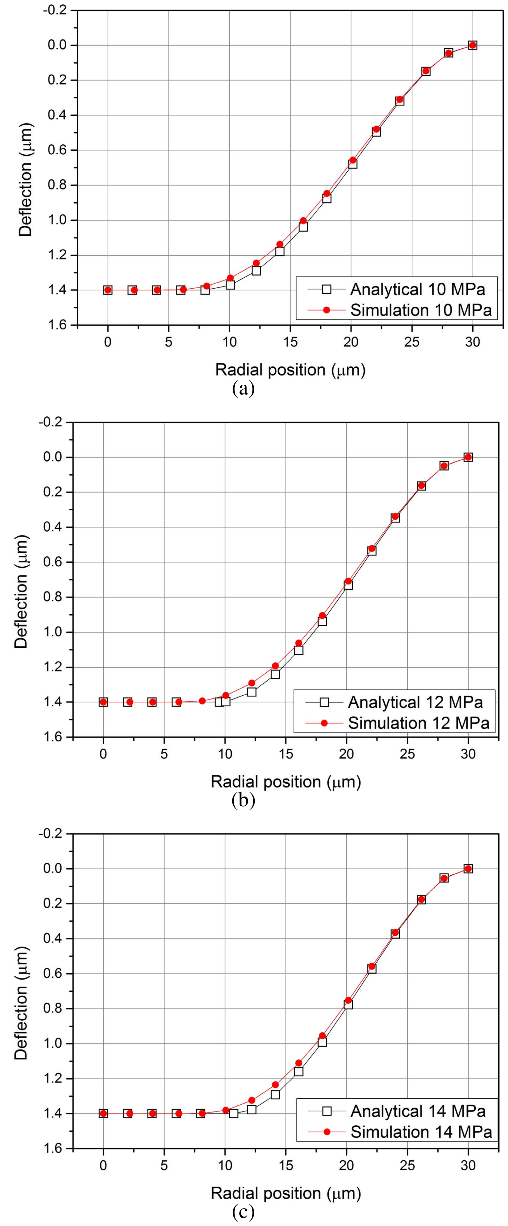

Fig. 6. Deflection profiles of the large deflection of membrane in collapse mode for (a) 10 MPa; (b) 12 MPa; and (c) 14 MPa pressures.

CMUT were obtained during the process. The calculation process to find the membrane displacement profile for the collapse CMUT requires longer computational time in comparison with the conventional CMUT. In our calculation, the typical computation times for evaluating the profiles of one conventional and one collapse mode cases on an Intel Core i7 (Dual core - 2.10 GHz, 2.69 GHz, 8 GB of RAM) computer were 0.18 s and 3.76 s, respectively.

The calculated membrane displacements and the associated results by FEM simulation using COMSOL are shown in Fig. 6. It should be emphasized that for the clarity of presentation, only cases of external pressure 10 MPa, 12 MPa, and 14 MPa are shown. The comparison between the results from calculation and also the FEM simulation for all ten cases (5 MPa to 14 MPa) reveals that the maximum error% of the

TABLE II
MAXIMUM DEFLECTION ERROR% OF LARGE DEFLECTION CASES IN COLLAPSE MODE

External Pressure, q	Error%
5 MPa	3.49%
6 MPa	3.81%
7 MPa	3.71%
8 MPa	3.72%
9 MPa	3.52%
10 MPa	3.61%
11 MPa	3.86%
12 MPa	4.12%
13 MPa	4.46%
14 MPa	4.67%

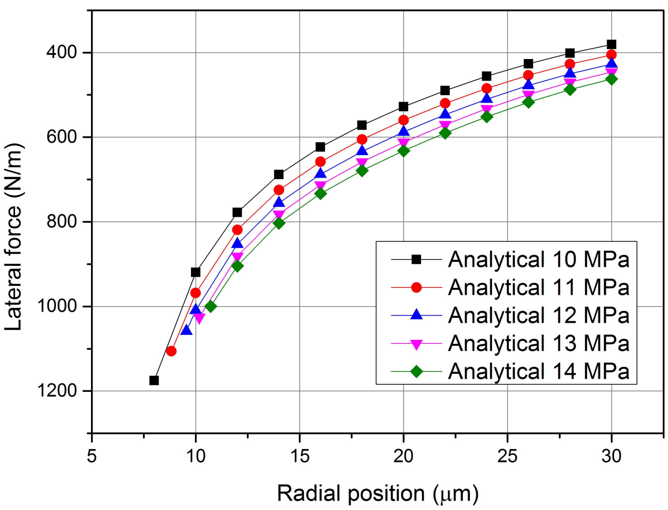

Fig. 7. Modeling results of the lateral force for the large deflection membranes in collapse mode.

membrane deflections is 4.7%, and the detailed difference for several pressure cases are in Table II. Similarly, the lateral forces for 10 MPa to 14 MPa on the membrane are also plotted in Fig. 7.

IV. COMPARISON AND DISCUSSION

In this section, the results related to the Section III are discussed here. The calculated lateral forces of the membrane for different cases are shown in Fig. 5 and Fig. 7. Theoretically, the lateral force is the stretching force coming from the elongation of the membrane, and can be expressed as (20) [24].

$$N_r = \frac{Eh}{1-\nu^2}\left[\frac{\mathrm{d}u}{\mathrm{d}r} + \frac{1}{2}\left(\frac{\mathrm{d}\varpi}{\mathrm{d}r}\right)^2 + \nu\frac{u}{r}\right] \tag{20}$$

As a result, a reaction force, which is caused by the lateral force and stiffness of the membrane, counteracts the external pressure and decreases the displacement of the membrane. With a higher external pressure, the elongation of the membrane u and ϖ are larger and the lateral force of the membrane fragment is higher.

For comparison, Fig. 8 shows the lateral force for small deflection cases using the similar parameters as in Table I except the pressures are 0.1 MPa $\sim$ 0.5 MPa. By comparing these figures, the trends of the lateral force are similar and increase with the external pressure. However, the membrane

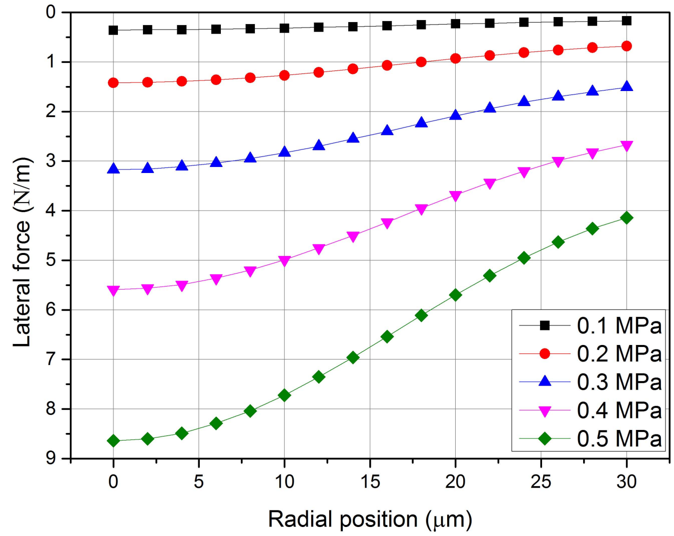

Fig. 8. Modeling results of the lateral force for the small deflection membranes in conventional mode.

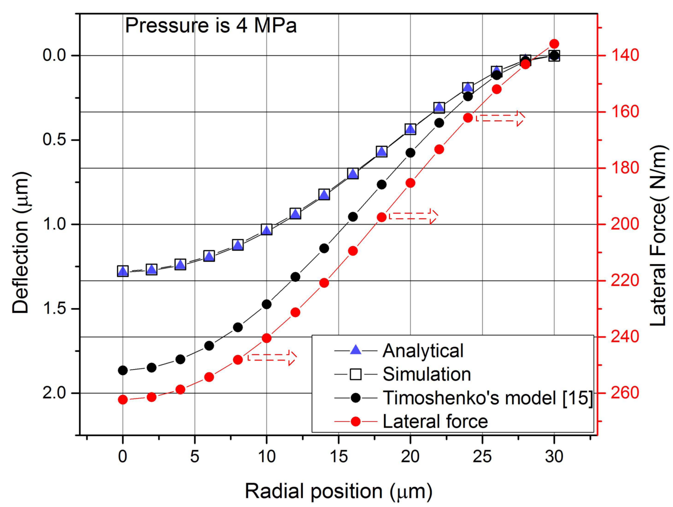

Fig. 9. Deflection profiles comparison, with corresponding lateral force using the right y-axis.

experienced less lateral force in small deflection than in large deflection cases. For small deflection cases, the effect of the lateral force is not notable and can be neglected for evaluating the displacement of the membrane. For example, in [12], [14], and [15], the proposed models without including the lateral force, still give quite accurate membrane displacements. On the contrary, by using the same Timoshenko's model [15] for large deflection case in conventional mode (same configuration in Section III-A with an external pressure of 4 MPa), the obtained membrane deflection profile deviates from the simulation result as depicted in Fig. 9. The figure shows the correlation with the lateral force and the difference between the Timoshenko's model adopted from [15] and the simulation result from FEM; the higher the lateral force, the larger the difference. With the introduction of the lateral force in the model proposed in this article, the displacement profile of the membrane matches well with the FEM simulation result.

Regarding to the collapse mode, the calculated displacement profiles have larger differences with the FEM results for 4.7%

when in comparison with the conventional mode for 1%. From the initial suggestion, the difference may be caused by neglecting the reaction force from the substrate to act on the collapse area of the membrane, which also contributes to the deformation of the overall membrane. Therefore, by properly introducing this supporting force at the collapse area in the future, the difference of the displacement profiles can be further reduced.

The model, as discussed previously, is developed for the consideration of the effects of the external pressure on the deformation of the membrane. For the CMUT in underwater vehicle, the external pressure on the membrane is changing in according to the water depth, e.g., the water pressure to the membrane is changing from 0.1 MPa to 10 MPa for 10 meters to 1000 meters deep. Depending on the configuration of the CMUT, its operating mode can change between conventional and collapse mode for different external pressures. For these applications, the proposed model can easily cover the scenarios and give accurate predictions of the membrane deflection profiles.

V. Conclusion

In this article, the authors proposed a mathematical approach to calculate the membrane deflection profile of the CMUT undergoing large deflection based on the Von Kármán Equations with the aid of the Perturbation Method. The comparisons between the calculated results and FEM simulation results for two typical CMUT operating modes, conventional and collapse, were discussed here. Additionally, the membrane deflection profiles and the effect of lateral force in each cases were also studied.

From the results, it was found that the lateral force cannot be neglected for a membrane undergone large deflection. Therefore, the proposed model with the consideration of the lateral force can give results closer to the FEM simulation for both operating modes of CMUTs. The maximum deflection errors of the proposed model were less than 1% & 4.7% in conventional & collapse modes, respectively. This more accurate model is specially useful for calculating the membrane deflection profile of the CMUT for underwater applications. Moreover, the current mathematical model can also be used for small deflection membranes in both conventional and collapse mode, which has similar performance in conventional mode CMUT but gives relatively larger error in collapse mode operation.

In the future, more complicated boundary conditions will be considered into the model to understand the behavior of laminated membranes covering different membrane structures and different coverage of top electrode. And the experimental results will be added when the device under fabrication is available.

Acknowledgment

The authors would like to express their appreciation for the valuable technical supports of Prof. Selim Olcum of MIT, Prof. Yuen Ka Veng and Mr. Lao Chi Kin of the University of Macau.

References

[1] J. L. Sutton, "Underwater acoustic imaging," *Proc. IEEE*, vol. 67, no. 4, pp. 554–566, Apr. 1979.
[2] O. Oralkan, A. S. Ergun, C.-H. Cheng, J. A. Johnson, M. Karaman, and B. T. Khuri-Yakub, "Underwater acoustic imaging using capacitive micromachined ultrasonic transducer arrays," in *Proc. OCEANS MTS/IEEE*, vol. 4, Oct. 2002, pp. 2354–2360.
[3] I. O. Wygant *et al.*, "Integration of 2D CMUT arrays with front-end electronics for volumetric ultrasound imaging," *IEEE Trans. Ultrason., Ferroelectr., Freq. Control*, vol. 55, no. 2, pp. 327–342, Feb. 2008.
[4] A. S. Ergun, G. G. Yaralioglu, and B. T. Khuri-Yakub, "Capacitive micromachined ultrasonic transducers: Theory and technology," *J. Aerosp. Eng.*, vol. 16, no. 2, pp. 76–84, Apr. 2003.
[5] S. Olcum *et al.*, "Wafer bonded capacitive micromachined underwater transducers," in *Proc. IEEE Ultrason. Symp.*, Sep. 2009, pp. 976–979.
[6] P. Cong, W. H. Ko, and D. J. Young, "Wireless batteryless implantable blood pressure monitoring microsystem for small laboratory animals," *IEEE Sensors J.*, vol. 10, no. 2, pp. 243–254, Feb. 2010.
[7] M. Shahiri-Tabarestani, B. A. Ganji, and R. Sabbaghi-Nadooshan, "Design and simulation of high sensitive capacitive pressure sensor with slotted diaphragm," in *Proc. Int. Conf. Biomed. Eng. (ICoBE)*, Feb. 2012, pp. 484–489.
[8] K.-S. Shin *et al.*, "Development of novel implantable intraocular pressure sensors to enhance the performance *in vivo* tests," *J. Microelectromech. Syst.*, vol. 24, no. 6, pp. 1896–1905, Dec. 2015.
[9] Y. Huang *et al.*, "Comparison of conventional and collapsed region operation of capacitive micromachined ultrasonic transducers," *IEEE Trans. Ultrason., Ferroelectr., Freq. Control*, vol. 53, no. 10, pp. 1918–1933, Oct. 2006.
[10] Y. Huang, X. Zhuang, E. O. Hæggstrom, A. S. Ergun, C.-C. Cheng, and B. T. Khuri-Yakub, "Capacitive micromachined ultrasonic transducers with piston-shaped membranes: Fabrication and experimental characterization," *IEEE Trans. Ultrason., Ferroelectr., Freq. Control*, vol. 56, no. 1, pp. 136–145, Jan. 2009.
[11] K. K. Park, O. Oralkan, and B. T. Khuri-Yakub, "Comparison of conventional and collapse-mode CMUT in 1-D array configuration," in *Proc. IEEE Ultrason. Symp.*, Oct. 2011, pp. 1000–1003.
[12] S. Olcum, F. Y. Yamaner, A. Bozkurt, H. Koymen, and A. Atalar, "An equivalent circuit model for transmitting capacitive micromachined ultrasonic transducers in collapse mode," *IEEE Trans. Ultrason., Ferroelectr., Freq. Control*, vol. 58, no. 7, pp. 1468–1477, Jul. 2011.
[13] B. Bayram, G. G. Yaralioglu, A. S. Ergun, and B. T. Khuri-Yakub, "Influence of the electrode size and location on the performance of a CMUT [US transducer]," in *Proc. IEEE Ultrason. Symp.*, vol. 2. Oct. 2001, pp. 949–952.
[14] A. Nikoozadeh, B. Bayram, G. G. Yaralioglu, and B. T. Khuri-Yakub, "Analytical calculation of collapse voltage of CMUT membrane [capacitive micromachined ultrasonic transducers]," in *Proc. IEEE Ultrason. Symp.*, vol. 1, Aug. 2004, pp. 256–259.
[15] S. Olcum, F. Y. Yamaner, A. Bozkurt, and A. Atalar, "Deep-collapse operation of capacitive micromachined ultrasonic transducers," *IEEE Trans. Ultrason., Ferroelectr., Freq. Control*, vol. 58, no. 11, pp. 2475–2483, Nov. 2011.
[16] I. O. Wygant, M. Kupnik, and B. T. Khuri-Yakub, "Analytically calculating membrane displacement and the equivalent circuit model of a circular CMUT cell," in *Proc. IEEE Ultrason. Symp.*, Nov. 2008, pp. 2111–2114.
[17] H. Koymen *et al.*, "An improved lumped element nonlinear circuit model for a circular CMUT cell," *IEEE Trans. Ultrason., Ferroelectr., Freq. Control*, vol. 59, no. 8, pp. 1791–1799, Aug. 2012.
[18] S. Satir, J. Zahorian, and F. L. Degertekin, "A large-signal model for CMUT arrays with arbitrary membrane geometry operating in non-collapsed mode," *IEEE Trans. Ultrason., Ferroelectr., Freq. Control*, vol. 60, no. 11, pp. 2426–2439, Nov. 2013.
[19] Y. Wei, E. Cretu, and R. Rohling, "Analytical modeling of CMUTs in coupled electro-mechano-acoustic domains using plate vibration theory," *IEEE Sensors J.*, vol. 11, no. 9, pp. 2159–2168, Sep. 2011.
[20] E. Ventsel and T. Krauthammer, *Thin Plates and Shells: Theory: Analysis, and Applications*. Boca Raton, FL, USA: CRC Press, 2001.
[21] A. Caronti, G. Caliano, A. Iula, and M. Pappalardo, "An accurate model for capacitive micromachined ultrasonic transducers," *IEEE Trans. Ultrason., Ferroelectr., Freq. Control*, vol. 49, no. 2, pp. 159–168, Feb. 2002.
[22] H. Koymen, M. N. Senlik, A. Atalar, and S. Olcum, "Parametric linear modeling of circular cMUT membranes in vacuum," *IEEE Trans. Ultrason., Ferroelectr., Freq. Control*, vol. 54, no. 6, pp. 1229–1239, Jun. 2007.

[23] H. Kagan Oguz, S. Olcum, M. N. Senlik, V. Tas, A. Atalar, and H. Koymen, "Nonlinear modeling of an immersed transmitting capacitive micromachined ultrasonic transducer for harmonic balance analysis," *IEEE Trans. Ultrason., Ferroelectr., Freq. Control*, vol. 57, no. 2, pp. 438–447, Feb. 2010.

[24] S. Timoshenko and S. Woinowsky-krieger, *Theory of Plates and Shells*. New York, NY, USA: McGraw-Hill, 1959.

[25] E. Aydogdu, A. Ozgurluk, A. Atalar, and H. Koymen, "Parametric nonlinear lumped element model for circular CMUTs in collapsed mode," *IEEE Trans. Ultrason., Ferroelectr., Freq. Control*, vol. 61, no. 1, pp. 173–181, Jan. 2014.

[26] M. Sheploak and J. Dugundji, "Large deflections of clamped circular plates under initial tension and transitions to membrane behavior," *J. Appl. Mech.*, vol. 65, no. 1, pp. 107–115, Mar. 1998.

[27] H. Xue and H. Hu, "Nonlinear characteristics of a circular plate piezoelectric harvester with relatively large deflection near resonance," *IEEE Trans. Ultrason., Ferroelectr., Freq. Control*, vol. 55, no. 9, pp. 2092–2096, Sep. 2008.

[28] C.-F. Chen and I.-W. Li, "Nonlinear mechanical sensitivity of unsymmetrically layered and pre-stressed piezoelectric plate in large deflection due to lateral load," in *Proc. IEEE SENSORS*, Nov. 2013, pp. 1–4.

[29] B. Bayram, E. Hæggstrom, G. G. Yaralioglu, and B. T. Khuri-Yakub, "A new regime for operating capacitive micromachined ultrasonic transducers," *IEEE Trans. Ultrason., Ferroelectr., Freq. Control*, vol. 50, no. 9, pp. 1184–1190, Sep. 2003.

[30] T.-Y. Huang, "On the large deflection of a circular plate with a circular hole at the center under uniform load," (in Chinese), *Acta Phys. Sin.*, vol. 13, no. 4, pp. 294–312, 1957.

[31] W.-Z. Chien, "Large deflection of a circular clamped plate under uniform pressure," *Acta Phys. Sin.*, vol. 7, no. 2, pp. 102–107, 1947.

[32] M. D. Van Dyke, *Perturbation Methods in Fluid Mechanics*. San Francisco, CA, USA: Academic, 1964.

[33] E. J. Hinch, *Perturbation Methods*. Cambridge, U.K.: Cambridge Univ. Press, 1991.

Jiujiang Wang (S'14) received the B.S. degree in microelectronic circuits and systems from the Beijing Institute of Technology, Beijing, China, in 1991, and the M.S. degree in semiconductor devices and microelectronics from the Institute of Semiconductors, Chinese Academy of Sciences, Beijing, China, in 1994. He is currently pursuing the Ph.D. degree in electrical and computer engineering with the University of Macau, Macau, China. He was a System Design Engineer with IC Company. His current research focuses on modeling and fabrication of CMUT devices.

Sio Hang Pun (S'11–A'12–M'12) received the master's degree in computer and electrical from the University of Porto, Portugal, in 1999, and the Ph.D. degree in electrical and electronics engineering from the University of Macau, Macau, in 2012.

He has been an Assistant Professor with the State Key Laboratory of Analog and Mixed-Signal VLSI, University of Macau, since 2012. His current research interests include biomedical electronic circuits, miniaturized sensors for biomedical applications, and human body communication.

Peng Un Mak (S'88–M'97–SM'11) received the B.Sc. degree from National Taiwan University, Taipei, Taiwan, and the M.Sc. and Ph.D. degrees from Michigan State University, East Lansing, MI, USA, all in electrical engineering. He has been the first Assistant Professor with the Department of Electrical and Computer Engineering, University of Macau, Macau, since 1997. He has authored or co-authored over 140 peer-reviewed technical publications (journal, book chapter, and conference proceeding). His current research interests are bio-signals extraction and processing, bio-electromagnetism, human body communication, miniaturized sensors, and body sensor network. He is also a member of Phi Kappa Phi and Eta Kappa Nu (now a.k.a. IEEE-HKN).

Ching-Hsiang Cheng (M'07) received the B.S. degree in mechanical engineering from National Taiwan University in 1993, three master's degrees in both electrical and mechanical engineering from Cornell University, Ithaca, NY, USA, in 1998, and the Ph.D. degree in electrical engineering from Stanford University in 2005. He held a post-doctoral research position with the Department of Mechanical Engineering, Stanford University. He joined the Mechanical and Systems Research Laboratories (MSL), Industrial Technology Research Institute, Taiwan, as a Researcher and became a Project Leader. In 2006, he was appointed as an Assistant Professor and also a Research Engineer with the Research Institute of Innovative Products and Technologies (RIIPT), The Hong Kong Polytechnic University (PolyU). In 2010, he joined the Department of Industrial and Systems Engineering, PolyU, as an Assistant Professor. His research interests include capacitive micromachined ultrasonic transducers, energy storage devices, shear and normal force sensors, large strain and tactile sensors, solar cells, microvalves and micropumps, gas sensors, electrical through-wafer interconnects, nanotechnology, and microelectromechanical systems.

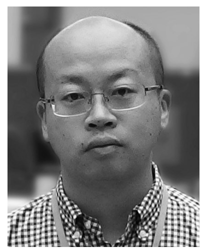

Yuanyu Yu (S'15) received the B.S. degree in biomedical engineering and the M.S. degree in measuring and testing technologies and instruments from the University of Electronic Science and Technology of China, Chengdu, China, in 2000 and 2005, respectively. He is currently pursuing the Ph.D. degree with the Department of Electrical and Computer Engineering, University of Macau, Macau, China. From 2005 to 2010, he was a System Design Engineer with Actions Semiconductor Company, Ltd. He has been a Research Fellow with the State Key Laboratory of Analog and Mixed-Signal VLSI of University of Macau since 2012. His research interests include design, modeling, and fabrication of CMUTs.

Pui-In Mak (S'00–M'08–SM'11) received the Ph.D. degree from the University of Macau (UM), Macao, China, in 2006. He is currently an Associate Professor with the UM Department of Electrical and Computer Engineering, Faculty of Science and Technology, and an Associate Director (Research) with the UM State Key Laboratory of Analog and Mixed-Signal VLSI. His research interests are on analog and radio-frequency (RF) circuits and systems for wireless, biomedical, and physical chemistry applications.

Dr. Mak served as an Editorial Board Member of IEEE Press (2014–2016), an IEEE Distinguished Lecturer (2014–2015), a Member of Board-of-Governors of IEEE Circuits and Systems Society (2009–2011), Senior Editor of the IEEE JOURNAL ON EMERGING AND SELECTED TOPICS IN CIRCUITS AND SYSTEMS (2014–2015), Guest Editor of the IEEE RFIC VIRTUAL JOURNAL (2014), an Associate Editor of the IEEE TRANSACTIONS ON CIRCUITS AND SYSTEMS I (2010–2011, 2014–2016), and the IEEE TRANSACTIONS ON CIRCUITS AND SYSTEMS II (2010–2013). He is the TPC Vice Co-Chair of ASP-DAC'16.

He (co)-received the DAC/ISSCC Student Paper Award in 2005, the CASS Outstanding Young Author Award in 2010, the SSCS Pre-Doctoral Achievement Awards in 2014 and 2015, the National Scientific and Technological Progress Award in 2011, and the Best Associate Editor of IEEE TRANSACTIONS ON CIRCUITS AND SYSTEMS II in 2012 and 2013. In 2005, He received the Honorary Title of Value for Scientific Merits by the Macau Government.

Mang I Vai (M'92–SM'06) received the Ph.D. degree in electrical and electronics engineering from the University of Macau, China, in 2002. Since 1984, he has been performing research in the areas of digital signal processing and embedded systems. He is currently the Co-ordinator with the State Key Laboratory of Analog and Mixed-Signal VLSI and an Associate Professor of Electrical and Computer Engineering, Faculty of Science and Technology, University of Macau.